Self-similarity and scaling of thermal shock fractures

S. Tarasovs[1] and A. Ghassemi[2]
[1]*Institute of Polymer Mechanics, University of Latvia, 23 Aizkraukles Street, Riga LV-1006, Latvia*
[2]*Mewbourne Department of Petroleum & Geological Engineering, University of Oklahoma, Norma, Oklahoma 73019, USA*
(Received 3 July 2013; revised manuscript received 23 June 2014; published 14 July 2014)

The problem of crack pattern formation due to thermal shock loading at the surface of half space is solved numerically using the two-dimensional boundary element method. The results of numerical simulations with 100–200 random simultaneously growing and interacting cracks are used to obtain scaling relations for crack length and spacing. The numerical results predict that such a process of pattern formation with quasistatic crack growth is not stable and at some point the excess energy leads to unstable propagation of one of the longest cracks. This single-crack scenario should be understood in a local sense. There could be other unstable cracks far away that together can form a new pattern. The onset of instability has also been determined from numerical results.

DOI: 10.1103/PhysRevE.90.012403 PACS number(s): 46.50.+a, 88.10.G−, 88.10.gn, 46.25.Hf

I. INTRODUCTION

The development of a hierarchical crack patterns is common in the failure of brittle material in response to loading by a thermal shock. The thermally induced stresses are released by the formation of an initial array of small cracks that grow in time as the cooling front propagates into the body, forming a system of cracks of different lengths. A similar process is the development of desiccation cracks in mud or paste drying [1–3] or columnar joint formation in cooling lava lakes [4–8]. Chemical decomposition of solids also can generate crack patterns [9,10]. Depending on the cooling and drying conditions, different crack patterns can be formed [11–16]. Many important characteristics of brittle solids such as fluid and heat transport properties depend on the number and length of the cracks; therefore, significant efforts were undertaken to develop the theory of thermal shock fracturing. In [17,18] the combination of strength theory and fracture mechanics was used to study the initiation and propagation of cracks due to the thermal shock of a brittle solid. The development of hierarchical crack patterns was explained in [19,20] by bifurcation instability analysis. In particular, it was concluded that at a certain length, the quasistatic propagation of an array of equidistant cracks becomes unstable and only every second crack continues to grow until a new instability point, where a reduced number of cracks would continue to propagate, is reached. The formation of a crack pattern in quenched glass or ceramic slabs was studied both experimentally and theoretically in [21–24].

Most of the existing studies of the hierarchical crack pattern formation used a simplified model of symmetric equidistant edge cracks. In real solids the locations of cracks at the moment of initiation are affected by the local variation in strength, so the generated crack pattern is not symmetric. However, it can be expected that, on average, the crack pattern that develops from such a random array of cracks has deterministic characteristics [25]. Only a few works have studied the formation of such random crack patterns. In [26] the crack pattern formation due to thermal shock loading was modeled using a simplified potential for crack growth and interaction and it was found that the average crack spacing does not depend on the initial crack configuration. Similar results were obtained in [27] using the two-dimensional boundary element method based on a complex hypersingular integral equation (CHIE) [28,29]. In this paper the CHIE method is used to simulate the simultaneous growth of many random cracks and to study the scaling relations that govern the formation of crack patterns resulting from instantaneous cooling of the surface of a half space. The CHIE method is an accurate and efficient way of solving problems dealing with cracks and crack propagation as demonstrated, e.g., in [30–32].

In the present work, two-dimensional boundary element method is used to build the numerical model of the formation of crack patterns that develop from an initial array of many small cracks randomly located at the surface of a half space in response to the thermal stress related to a nonstationary thermal field. The numerical modeling accounts for the mechanical interaction of growing cracks and the arrest of some of the cracks, followed by the formation of a hierarchical pattern. Such numerically generated crack patterns are used to study the scaling laws that characterize the length and average density of the thermally driven cracks.

II. THERMAL CRACKING OF THE SURFACE OF HALF SPACE

A. Single crack

Before considering the propagation of many cracks under thermal stress, it is useful to study the behavior of a single crack and its growth in time under thermal stress. Consider a half space with an initial temperature T_0, subjected to instant cooling at its surface using a temperature drop of $\Delta T = T_0 - T_S$, where T_S is the half-space surface temperature. The problem can be solved analytically and the temperature profile at any moment in time equals [33]

$$T(z) = T_0 - \Delta T \,\mathrm{erfc}\left(\frac{z}{L}\right), \tag{1}$$

where z is the distance from the surface, L is the cooling depth, which equals $L = \sqrt{4t\kappa}$, t is time, and κ is the thermal diffusivity of the solid. The cooling of the surface creates a thermally induced stress in the material and for the two-dimensional plane strain condition, the tangential thermal stress component is given by

$$\sigma_{th}(z) = \frac{E\alpha[T_0 - T(z)]}{1-\nu}, \tag{2}$$

where E is Young's modulus, ν is Poisson's ratio, and α is the coefficient of linear thermal expansion.

The process of crack growth due to the thermal shock loading has two intrinsic length scales: the depth of the cooling zone L and the characteristic length of the material ξ, defined as

$$\xi \equiv \left(\frac{K_{Ic}(1-\nu)}{E\alpha\Delta T}\right)^2, \tag{3}$$

with K_{Ic} being the fracture toughness of the material. The characteristic length ξ is the ratio of the energy required to create a new crack surface and the thermoelastic energy that is generated in the solid by the thermal shock. From dimensional considerations the stress intensity factor (SIF) at the tip of a single edge crack of length a, normal to the solid surface, and loaded by thermally induced stress can be expressed as

$$K_I = \frac{E\alpha\Delta T}{1-\nu}\frac{L}{\sqrt{a}} f\left(\frac{a}{L}\right), \tag{4}$$

where the nondimensional function f has to be determined numerically and can be approximated as

$$f\left(\frac{a}{L}\right) = 0.87\tanh\left(2.2\frac{a}{L}\right). \tag{5}$$

For short cracks, i.e., when $a/L < 0.5$, the SIF is approximately proportional to $\sqrt{a}$ and such a crack is unstable. For long cracks (when $a/L > 1$) the function f is approximately constant and the crack length can be estimated as

$$a = \left(0.87\frac{E\alpha\Delta T}{K_{Ic}(1-\nu)}\right)^2 L^2. \tag{6}$$

Therefore, as $L = \sqrt{4t\kappa}$, the length of the single crack subjected to thermal shock is a linear function of time.

B. Array of random cracks

To study the process of an interaction of many cracks, we start the simulations from an initial array of many small cracks with length a_0 and average spacing d_0, as shown in Fig. 1. Using the superposition principle, the thermal load is applied at the faces of the cracks. The randomness of the initial crack array is introduced via perturbations in the cracks locations: Each initial crack is shifted from its position by a random value $\pm\Delta d$, keeping the average spacing between the cracks d_0 constant. The simulation results show that after several crack increments, when some of the initial cracks stop, the resulting crack pattern does not depend on the initial geometry in the average sense, so the crack spacing follows a single curve irrespective of the initial crack's configuration. To replicate a large number of cracks, an initial array of 100–200 small cracks with periodic boundary conditions (so that the whole random array is repeated) was used in the simulations. For accurate determination of the resulting average crack spacing, normally about six independent simulations with different random crack locations were performed for each value of characteristic length ξ.

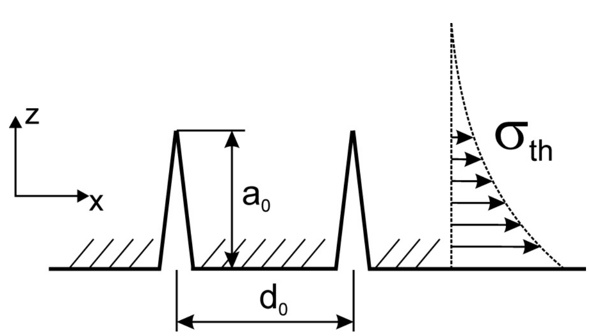

FIG. 1. Array of edge cracks with length a_0 and spacing d_0, subjected to the thermally induced stresses $\sigma\uparrow_{\rm th}$.

The cracks propagate when the stress intensity factor at their tips exceeds the fracture toughness of the material K_{Ic}. The propagation criterion is applied to every crack tip at every time step and if the criterion is fulfilled, the cracks are advanced by a small increment. The propagation angle is chosen according to the principle of local symmetry: The crack grows along the path where the stress intensity factor in mode II equals zero ($K_{\rm II} = 0$). The algorithm suggested in [34] is used in the present work to find the propagation angle simultaneously for all advancing crack tips.

The crack patterns for different values of normalized initial crack spacing d_0/ξ are presented in Fig. 2. As one of the cracks stops growing, the neighboring cracks change their direction of propagation, redistributing evenly in space. The numerical results suggest that the process of crack pattern formation is self-similar, i.e., the crack pattern repeats itself on different time and length scales. The results of simulations, i.e., the maximum crack length (the length of the longest crack at a given time) and average crack spacing (measured at a given depth z at the end of the simulation when all shorter cracks are arrested and do not grow) normalized with respect to the material constant ξ, are presented in Figs. 3 and 4 on a logarithmic scale. The power-law curve fits shown correspond to Eqs. (7) and (8), respectively:

$$\frac{a}{\xi} = 1.1\left(\frac{L}{\xi}\right)^{1.075\pm0.005}, \tag{7}$$

$$\frac{d}{\xi} = 5.5\left(\frac{z}{\xi}\right)^{0.74\pm0.01}. \tag{8}$$

C. Cooling the surface of a body subject to stress

Let us assume that the instantly cooled surface is that of a body subjected to a compressive stress σ_∞ (compression is considered negative) applied at infinity. Such compressive stress could be the *in situ* stress in earth's crust or the residual stress often observed in material coatings. We assume that the absolute value of the compressive stress is smaller than maximum thermal stresses at the surface $[E\alpha\Delta T/(1-\nu)]$, so there is a zone of tensile stress near the surface that changes to compressive stress deeper in the body. It could be expected that cracks will not penetrate the compressive zone and the crack pattern is mainly governed by the shape of the temperature profile in the tensile region near the surface. The shape of

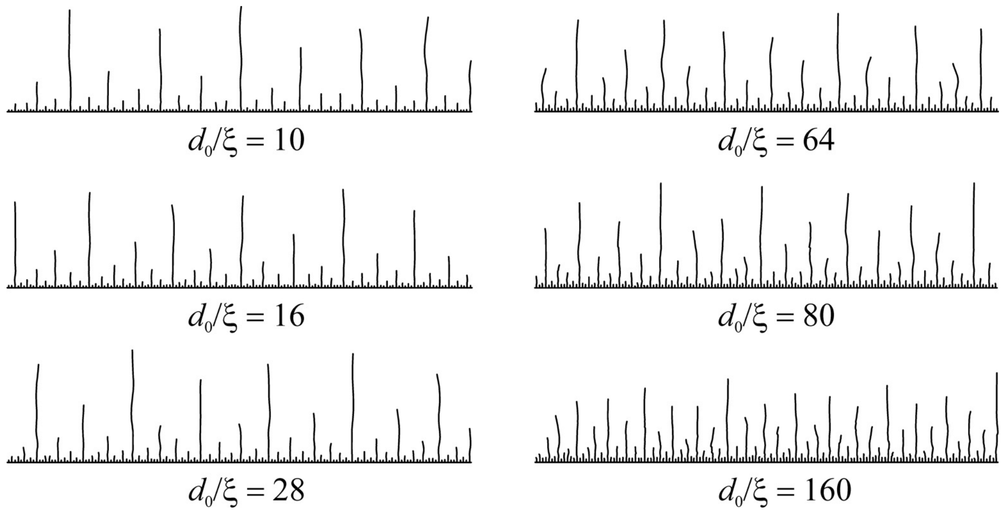

FIG. 2. Crack patterns formed in simulations of thermal shock fracture with different values of normalized initial crack spacing d_0/ξ. The length scales and time are different in each figure, but the pattern development in time is similar.

the stress profile now depends on the ratio of the compressive stresses to the thermal stresses at the surface $\lambda = |\sigma_\infty| / \sigma_{th}(0)$. For $\lambda = 0$, the scaling law (8) can be applied for crack spacing. However, as λ tends to unity, the stress profile in the tensile zone becomes closer to a linear function as shown in Fig. 5.

For simplicity, the linear temperature distribution was chosen as

$$T(z) = \begin{cases} T_0 - \Delta T \frac{L-z}{L}, & 0 \leqslant z < L \\ T_0, & z \geqslant L. \end{cases} \tag{9}$$

The results show that scaling laws of the crack pattern for a linear temperature distribution are different from scaling laws for an error-function distribution. In the case of a linear temperature profile, the crack length does not depend on the material's fracture toughness and the length of the longest crack is always approximately equal to the cooling depth L:

$$a = L. \tag{10}$$

The crack spacing, however, does depend on fracture toughness and can be approximated by a power-law scaling similar to Eq. (8):

$$\frac{d}{\xi} = 5.8 \left(\frac{z}{\xi}\right)^{0.59\pm0.01}. \tag{11}$$

These scaling relations are also presented in Figs. 3 and 4 together with those for the case of instant cooling of the surface. As will be shown in the next section, there exists a smooth transition from one scaling law to another as the temperature profile changes from an error function to a linear function.

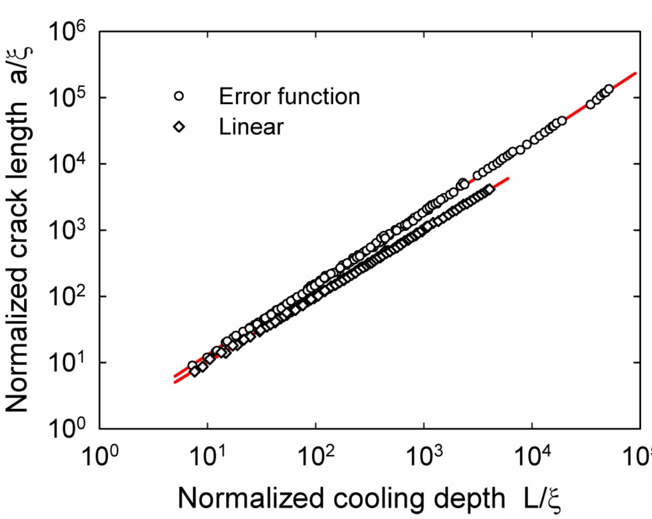

FIG. 3. (Color online) Scaling relation between maximal crack length a (length of the longest crack at given time) and cooling depth L for two shapes of temperature profile. Symbols represent the numerical results and lines show the power-law fit [Eqs. (7) and (10)].

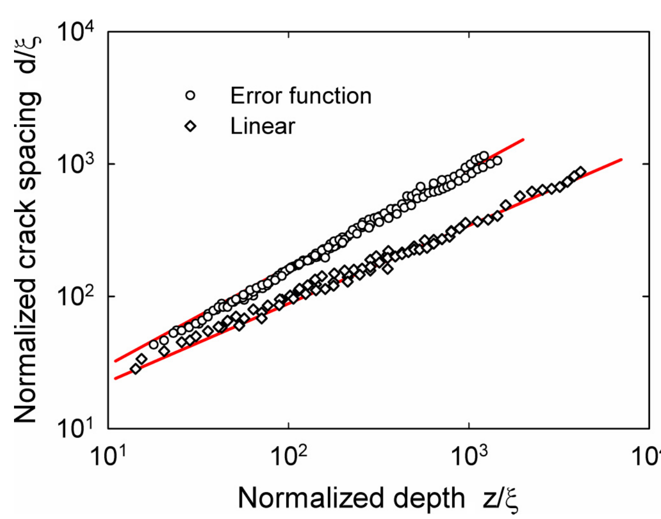

FIG. 4. (Color online) Scaling relation between crack spacing d and depth for two shapes of temperature profile. Symbols represent the average numerical results and lines show the power-law fit [Eqs. (8) and (11)].

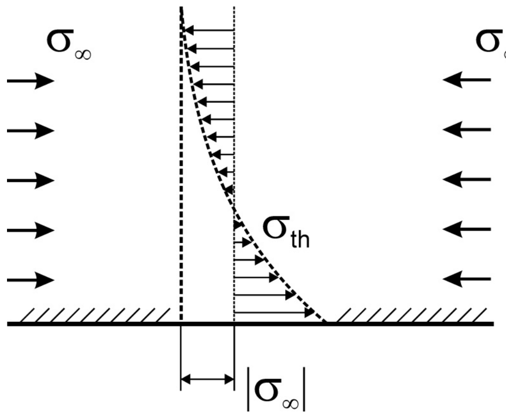

FIG. 5. Stress profile near the surface for simultaneous action of tensile thermally induced stress and a compressive far-field stress.

In the case of simultaneous action of thermal stress and a compressive far-field stress, the characteristic length scale can be defined as

$$\eta \equiv \left(\frac{K_{Ic}}{E\alpha\Delta T/(1-\nu)+\sigma_\infty}\right)^2. \quad (12)$$

It could be expected that by changing the fracture toughness and keeping the stress ratio (parameter λ) constant, a single scaling law should be obtained. In contrast, by changing the confining stress σ_∞ and thus changing the shape of the stress profile different scaling laws should be obtained with exponent values between 0.59 and 0.74 (corresponding to the two temperature profiles considered previously). The normalized crack spacing for these two cases is presented in Fig. 6. The red lines present the scaling for two extreme cases: the error function (8) and the linear (11) temperature profile. Figure 6(a) presents the normalized crack spacing of four different simulations using different fracture toughness values but with the same stress ratio parameter $\lambda = 0.5$ (the corresponding values of characteristic length scale η are shown in figure). Figure 6(b) presents results of simulations with the stress ratio parameter λ equal to 0.0825, 0.25, and 0.625 with scaling exponents equal to 0.66, 0.64, and 0.60, respectively. As could be expected, the scaling exponent depends on the stress profile, with a smooth transition between 0.74 and 0.59 corresponding to the error function and linear profile, respectively.

The length of the cracks in the case of an existing compressive stress can be estimated using the assumption that thermally driven cracks do not propagate into the compressive zone. To simplify the analysis, the actual temperature profile can be replaced by an equivalent parabolic profile [19]

$$T(z) = \begin{cases} T_0 - \Delta T\left(1-\frac{z}{\sqrt{3}L}\right)^2, & 0 \leqslant z < \sqrt{3}L \\ T_0, & z \geqslant \sqrt{3}L. \end{cases} \quad (13)$$

Then the maximum cracks length can be found from the condition $\sigma_{th} + \sigma_\infty = 0$, which gives [35]

$$a = \sqrt{3}L\left(1-\sqrt{-\frac{\sigma_\infty(1-\nu)}{E\alpha\Delta T}}\right). \quad (14)$$

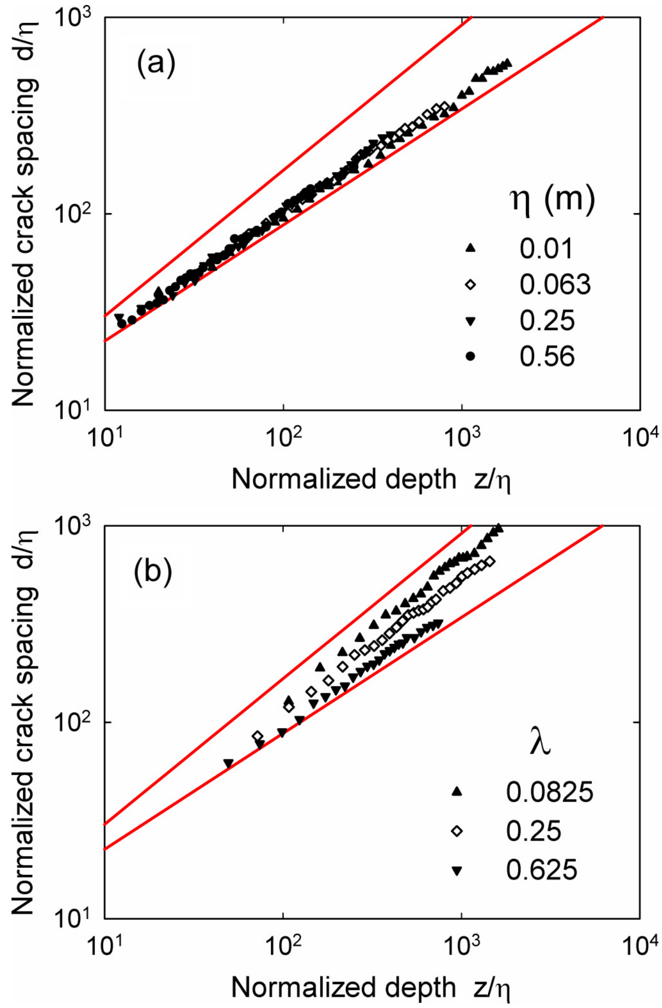

FIG. 6. (Color online) Average crack spacing in the presence of confining compressing stresses. Results are shown for (a) $\lambda = 0.5$ and four different characteristic length scales η and (b) $\lambda = 0.0825$, 0.25, and 0.625.

III. STABILITY OF CRACK GROWTH

From Eq. (7) it follows that the depth of the random array of thermal cracks for the instantaneous cooling of a half space is approximately proportional to the square root of time. It should be noted that the scaling laws (7) and (8) are quite close to those derived in [36] based on a simplified bifurcation analysis that resulted in a simple relation between the crack length and spacing $ad = 1.74L^2$ [36]. Combining Eqs. (7) and (8) yields $ad = 6\xi^{0.13}L^{1.87}$ for our analysis. The scaling relation for crack spacing in [36] is not a power function, but the numerical values for the normalized depth in the range 10^1–10^4 are quite close to those obtained in our work. Outside this range, the solution is not physically meaningful. For $a/\xi < 10$, a crack initiation criterion has to be applied to determine the smallest possible crack size and spacing. Such an analysis [37,25] shows that the initial crack length is of the order of ξ. A theoretical limit for the crack spacing was obtained in [25] using the known solution for the stress intensity factor for an array of long cracks with spacing equal d in a uniform stress field $K = \sigma\sqrt{0.5d}$. It immediately follows from this solution that the theoretical minimum normalized spacing d/ξ equals 2. In [37] the formation of the system of cracks in the shrinking slab was studied using the energy minimization principle. It was found that for a thick slab, which corresponds to the semi-infinite body studied in the present work, the minimum initial normalized crack spacing approximately equals 8. In our work an arbitrary system of initial cracks can be generated at the beginning of simulations; however, it was observed that for the stable evolution of such a crack system the normalized crack spacing should be ≥ 10. For smaller spacing most of the initial cracks will not advance at all, indicating that such an initial configuration is not physical. Therefore, the scaling laws (7) and (8) can be applied only after the initial cracks advance and begin to interact.

For the long-range values of normalized crack length the numerical solution becomes unstable. The nature of this instability can be explored by considering the elastic energy of the system. The elastic energy induced in the body by cooling is proportional to the cooling depth L. Using relations (7) and (8), the total length of all cracks per unit length of the cooled surface can be estimated as

$$S_{\text{total}} = \int_0^a \frac{1}{d} dz \sim \xi^{-0.28} L^{0.28}. \tag{15}$$

Equation (15) predicts that the total length of all cracks grows much slower than the cooling-induced elastic energy. The excess energy is accumulated in the system and this energy eventually may be released by the unstable growth of some cracks. Physically, this means that at some stage of propagation, the classical alternating bifurcation solution [19,20], where every second crack stops at the bifurcation point, is no longer favorable and it is replaced by another solution with only a single growing crack. The unstable growth of one crack was observed in all numerical simulations where the simulation time was sufficiently large. There is a possibility that other cracks may start to grow unstably far away so that these cracks do not interact with each other, resulting in the formation of a new pattern in the future; however, this was not observed in numerical simulations due to the limited size of the domain.

The global energy analysis only shows the possibility of unstable growth of the cracks. For a more detailed analysis of instability, a particular simulation was stopped at three different times $t_1 < t_2 < t_3$ and one of the longest cracks was manually extended, keeping all other cracks and the temperature profile constant. The stress intensity factor of the manually extended crack is plotted in Fig. 7. The results show that the crack is stable at early times and the SIF decreases with a small extension of the crack and then starts to increase again for larger crack extensions. However, at later times the behavior changes and crack becomes unstable and the SIF increases even for small increments of the crack growth. Similar behavior was observed for other cracks, but eventually only one crack dominates and starts to grow unstably, suppressing the growth of other cracks.

In Eq. (15) we have assumed that an infinite number of infinitesimal cracks exist. Since in both real materials and numerical simulations the process of thermal shock cracking starts from an initial array of cracks with finite lengths, the onset of instability depends on the initial configuration, i.e., the initial crack length and initial spacing. However, assuming that at the beginning of simulations all cracks have subcritical length, in other words, in the first time increments all cracks grow in a stable manner until the first bifurcation point is reached, only one remaining geometrical parameter may control the crack pattern evolution: the initial spacing between cracks.

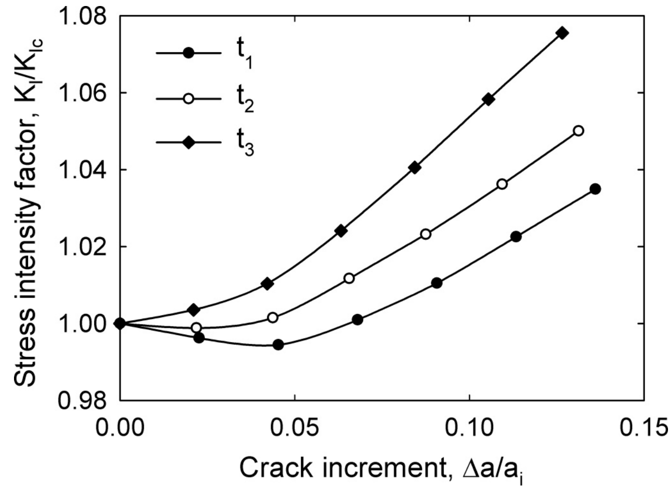

FIG. 7. Stress intensity factor of an extended crack at three different time moments $t_1 < t_2 < t_3$.

The critical crack length at the onset of instability shows a strong correlation with the normalized initial spacing d_0/ξ and can be approximated by a power-law function

$$\frac{a_{cr}}{\xi} = 90\left(\frac{d_0}{\xi}\right)^{0.72\pm0.01}. \tag{16}$$

The critical crack length is plotted in Fig. 8 together with the power-law fit. It should be noted that the limited size of the domain in the numerical simulations may impact the instability onset, but we did not observe any dependence on either the

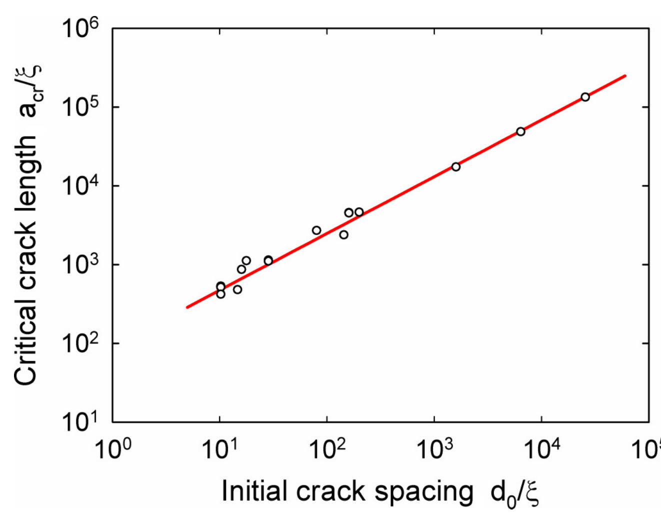

FIG. 8. (Color online) Onset of instability during quasistatic growth of an array of edge cracks. Symbols represent the numerical results and the line shows the power-law fit.

number of initial cracks, e.g., from 50 to 200, or the span of the simulated domain.

IV. CONCLUSION

Extensive two-dimensional numerical simulations of crack propagation under thermal shock have been performed using the complex variable hypersingular boundary element method with a periodic array of about 100–200 simultaneously growing random cracks. The numerical results have shown that the crack pattern is self-similar. The scaling relations for the crack length and crack spacing were obtained by analyzing the numerically simulated patterns. It has been found that the scaling exponent depends on the actual shape of the temperature profile and there is a smooth transition in scaling laws as the temperature profile changes from an error function to a linear function. It was found that the total length of all cracks grows much slower than the strain energy of the thermal stress due to cooling. This excess energy may lead to the unstable propagation of some cracks. Such a process has been observed in numerical simulations and has been used to determine the onset of instability.

ACKNOWLEDGMENTS

This project was supported by the US Department of Energy Office of Energy Efficiency and Renewable Energy under Cooperative Agreement No. DE-PS36-08GO1896. This support does not constitute an endorsement by the US Department of Energy of the views expressed in this publication. The authors thank anonymous reviewers for their valuable comments and suggestions that improved the paper. Also, S.T. gratefully acknowledges Dr. J. Andersons of Institute of Polymer Mechanics, Latvia, for helpful discussions.

[1] K.-t. Leung and Z. Néda, Phys. Rev. Lett. **85**, 662 (2000).
[2] J. Bisschop, Int. J. Fract. **154**, 211 (2008).
[3] T. Hornig, I. M. Sokolov, and A. Blumen, Phys. Rev. E **54**, 4293 (1996).
[4] L. Goehring, S. W. Morris, and Z. Lin, Phys. Rev. E **74**, 036115 (2006).
[5] L. Goehring, L. Mahadevan, and S. W. Morris, Proc. Natl. Acad. Sci. USA **106**, 387 (2009).
[6] E. A. Jagla and A. G. Rojo, Phys. Rev. E **65**, 026203 (2002).
[7] A. Nishimoto, T. Mizuguchi, and S. Kitsunezaki, Phys. Rev. E **76**, 016102 (2007).
[8] M. Hofmann, H.-A. Bahr, H.-J. Weiss, U. Bahr, and H. Balke, Phys. Rev. E **83**, 036104 (2011).
[9] B. I. Yakobson, Phys. Rev. Lett. **67**, 1590 (1991).
[10] A. Malthe-Sørenssen, B. Jamtveit, and P. Meakin, Phys. Rev. Lett. **96**, 245501 (2006).
[11] E. A. Jagla, Phys. Rev. E **65**, 046147 (2002).
[12] T. Boeck, H.-A. Bahr, S. Lampenscherf, and U. Bahr, Phys. Rev. E **59**, 1408 (1999).
[13] E. R. Dufresne, E. I. Corwin, N. A. Greenblatt, J. Ashmore, D. Y. Wang, A. D. Dinsmore, J. X. Cheng, X. S. Xie, J. W. Hutchinson, and D. A. Weitz, Phys. Rev. Lett. **91**, 224501 (2003).
[14] E. R. Dufresne, D. J. Stark, N. A. Greenblatt, J. X. Cheng, J. W. Hutchinson, L. Mahadevan, and D. A. Weitz, Langmuir **22**, 7144 (2006).
[15] Y. Hayakawa, Phys. Rev. E **50**, R1748 (1994).
[16] L. Pauchard, M. Adda-Bedia, C. Allain, and Y. Couder, Phys. Rev. E **67**, 027103 (2003).
[17] D. P. H. Hasselman, J. Am. Ceram. Soc. **46**, 535 (1963).
[18] D. P. H. Hasselman, J. Am. Ceram. Soc. **52**, 600 (1969).
[19] Z. P. Bažant, H. Ohtsubo, and K. Aoh, Int. J. Fract. **15**, 443 (1979).
[20] S. Nemat-Nasser, L. M. Keer, and K. S. Parihar, Int. J. Solids Struct. **14**, 409 (1978).
[21] J. F. Geyer and S. Nemat-Nasser, Int. J. Solids Struct. **18**, 349 (1982).
[22] H.-A. Bahr, G. Fischer, and H.-J. Weiss, J. Mater. Sci. **21**, 2716 (1986).
[23] H.-A. Bahr and H.-J. Weiss, Theor. Appl. Fract. Mech. **6**, 57 (1986).
[24] H.-A. Bahr, H.-J. Weiss, H. G. Maschke, and F. Meissner, Theor. Appl. Fract. Mech. **10**, 219 (1988).
[25] Y. N. Li, A. Hong, and Z. Bazant, Int. J. Fract. **69**, 357 (1995).
[26] H.-A. Bahr, U. Bahr, and A. Petzold, Europhys. Lett. **19**, 485 (1992).
[27] S. Tarasovs and A. Ghassemi, Geotherm. Res. Council Trans. **34**, 463 (2010).
[28] A. M. Linkov and S. G. Mogilevskaya, Acta Mech. **105**, 189 (1994).
[29] A. M. Linkov, *Boundary Integral Equations in Elasticity Theory* (Kluwer Academic, Dordrecht, 2002).
[30] V. Koshelev and A. Ghassemi, J. Eng. Anal. Bound. Elem. **28**, 825 (2004).
[31] A. A. Dobroskok, A. Ghassemi, and A. M. Linkov, Int. J. Fract. **133**, 223 (2005)
[32] A. Koshelev and A. Ghassemi, J. Eng. Anal. Bound. Elem. **32**, 168 (2008).
[33] H. S. Carslaw and J. C. Jaeger, *Conduction Of Heat In Solids*, 2nd ed. (Clarendon, Oxford, 1959).
[34] T. J. Stone and I. Babuška, Comput. Methods Appl. Mech. Eng. **160**, 245 (1998).
[35] S. Tarasovs and A. Ghassemi, in *Proceedings of 45th U.S. Rock Mechanics/Geomechanics Symposium, San Francisco, 2011* (American Rock Mechanics Association, Alexandria, 2011), p. 6.
[36] H.-A. Bahr *et al.*, J. Mech. Phys. Solids **58**, 1411 (2010).
[37] D. R. Jenkins, Phys. Rev. E **71**, 056117 (2005).